Hindawi
International Journal of Aerospace Engineering
Volume 2020, Article ID 8896357, 15 pages
https://doi.org/10.1155/2020/8896357

Research Article

Rapid Penetration Path Planning Method for Stealth UAV in Complex Environment with BB Threats

Zhe Zhang,[1] **Jian Wu**,[1,2] **Jiyang Dai**,[1] **and Cheng He**[1]

[1]*School of Information Engineering, Nanchang Hangkong University, Nanchang 330063, China*
[2]*School of Reliability and System Engineering, Beihang University, Beijing 100191, China*

Correspondence should be addressed to Jian Wu; wujiannchu@126.com

Received 16 June 2020; Revised 5 July 2020; Accepted 8 July 2020; Published 1 August 2020

Academic Editor: Hikmat Asadov

This paper presents the flight penetration path planning algorithm in a complex environment with Bogie or Bandit (BB) threats for stealth unmanned aerial vehicle (UAV). The emergence of rigorous air defense radar net necessitates efficient flight path planning and replanning for stealth UAV concerning survivability and penetration ability. We propose the improved A-Star algorithm based on the multiple step search approach to deal with this uprising problem. The objective is to achieve rapid penetration path planning for stealth UAV in a complex environment. Firstly, the combination of single-base radar, dual-base radar, and BB threats is adopted to different threat scenarios which are closer to the real combat environment. Besides, the multistep search strategy, the prediction technique, and path planning algorithm are developed for stealth UAV to deal with BB threats and achieve the penetration path replanning in complex scenarios. Moreover, the attitude angle information is integrated into the flight path which can meet real flight requirements for stealth UAV. The theoretical analysis and numerical results prove the validity of our method.

1. Introduction

1.1. Background and Motivation. In recent years, the emergence of new military equipment and systems, the stealth unmanned aerial vehicles (UAV) are gaining much attention due to the air-defense radar net is increasingly in the field of close and low altitude combat. Meanwhile, the survivability and combat effectiveness of stealth UAV will have a great influence on modern air warfare [1, 2]. The nose, fuselage, and tail of stealth UAV have relatively small radar cross-section (RCS), which aims to reduce the detection probability of radar system and improve the penetration ability and survivability of the stealth UAV [3]. However, previous works have mainly concentrated on the path planning in the static environment, there are many theoretical challenges and practical problems for stealth UAV on the problem of penetration path planning, such as the constraint of attitude angle and control of track point, the efficiency of path planning algorithm, and real-time performance. Besides, with regard to the Bogie or Bandit (BB) threats in the real combat environment, it is difficult for stealth UAV to achieve penetration path planning which is rapidly and safely. Therefore, the kinematics model and path planning algorithm for stealth UAV should be studied in a complex environment.

1.2. Literature Review. More recently, a lot of research has been done in the area of penetration path planning for aircraft, and so many algorithms had been proposed. In Reference [4], a new concept on the aircraft path planning for the variation of radar cross-section (RCS) was firstly presented, which indicates that the stealth UAV can significantly reduce the RCS by adjusting the attitude angle. In Reference [5], a research framework of low detectability tactical trajectory planning was proposed in the presence of multiple radar-detected threat environments; the solution of the optimal trajectory is transformed into the optimal control problem with the minimum radar detection probability. A penetration trajectory optimization method considering the influence of aircraft radar RCS was proposed in Reference [6]. In Reference [7] and Reference [8], a hybrid heuristic adaptive pseudospectrum method was proposed to address the low-detectability trajectory planning problem. In contrast, these methods usually adopt a simplified kinematic model, which aims to obtain a rough reference track, and

the constraints and control conditions of radar attitude are rarely considered in the reference trajectories. In Reference [9], a path planning method for stealth UAV based on the RCS ellipsoid model was proposed to find the optimal trajectory during flight. Inversely, this model requires a large amount of computation in addressing the problem of path planning. In Reference [10], a trajectory planning method based on dynamic game theory was presented to analyze the relationship between radar and UAV. In Reference [11], a real-time air battle trajectory optimization and game model for aircraft based on a rolling time-domain control strategy were proposed in a complex environment. However, two kinds of shortages exist in the research. One was that only can be applied to the static environment with known radar position, and it rarely achieves the path planning for stealth UAV in the dynamic environment. The other was that the calculation process is relatively complicated, and the real-time performance of the path planning method is poor. Erlandsson proposed a path planning model, and the expected path cost of air mission was discussed in a hostile environment; the particle swarm optimization algorithm (PSO) was adopted to address the optimization path planning problem [12, 13]. Meanwhile, many scholars are focus on analyzing a series of optimization algorithms to address the penetration path planning problem for unmanned aerial vehicle, such as A-Star algorithm [14], genetic algorithms (GA) [15], sparse A-Star algorithm (SAS) [16], rapidly exploring random-tree algorithm (RRT) [17, 18], particle swarm optimization algorithm (PSO) [19, 20], black hole algorithm [21], and other combinatorial optimization algorithms [22]. However, these optimization algorithms are only applied to address the stealth path planning problem in the static combat environment, the single-base radar is usually adopted in the combat scenario that the position of each radar is known, and the number is relatively small. Furthermore, the efficiency of the algorithm and the safety of the path are rarely optimal.

1.3. Contribution. In this paper, we focus on analyzing the penetration path planning for stealth UAV based on an improved A-Star algorithm, which aims to achieve rapid penetration path planning in the dynamic combat environment with BB threats. The novelty of this method is summarized as follows: firstly, the main idea of the model-based predictive control (MPC) and learning real-time A-Star algorithm (LRTA) is integrated into the path to devise the improved A-Star algorithm. Additionally, for the BB threats in a complex environment, the improved A-Star algorithm is applied for the penetration path replanning with fixed altitude to improve the survivability and combat effectiveness of stealth UAV. Moreover, numerical simulation results are applied to demonstrate the validity of the improved A-Star algorithm in the presence of the radar net with BB threats.

1.4. Paper Organization. The paper is organized as follows. Section 2 describes the mathematical model of stealth UAV. Section 3 discusses the detection probability calculation of multiple radar net, which is close to the real combat environment. Section 4 presents the improvement of the path planning algorithm, includes improved A-Star algorithm, LRTA-Star algorithm, and D-Star algorithm. Our numerical results and evaluation are presented in Section 5. Section 6 states our conclusions and future work.

2. The System Modeling

2.1. Kinematics. It is assumed that the stealth UAV can be defined as a particle with attitude information and ignores the influence of wind and other external conditions [1]. We are focus on studying the control of the flight path. The stealth UAV moves in a horizontal plane at a constant altitude h. Therefore, the kinematics model can be given by

$$\begin{cases} \dot{x} = v\cos\varphi \\ \dot{y} = v\sin\varphi \\ \dot{\varphi} = \dfrac{u}{v} \end{cases}, \tag{1}$$

where x and y are the Cartesian coordinates of the aircraft, φ is the heading angle, v is the constant speed, u is the input signal, and is the acceleration normal to the flight path vector.

Specify radar locations in the plane $h = 0$ (on the ground) by the coordinates $(x_i, y_i, 0)$. The range from the ith radar to the stealth UAV is given by

$$R_i = \sqrt{(x - x_i)^2 + (y - y_i)^2 + h^2}. \tag{2}$$

Additionally, let

$$\begin{cases} \alpha_i = \arctan\left(\dfrac{y - y_i}{x - x_i}\right) \\ \lambda_i = \alpha_i - \varphi + \pi \\ \theta = \arctan\left(\dfrac{u}{g}\right) \end{cases}, \tag{3}$$

be the azimuth, aspect, and roll angles, respectively, measured to the ith radar, g is the acceleration of gravity.

2.2. Dynamic RCS Features. Radar cross-section (RCS) is a measure of ability for UAV to reflect electromagnetic radiation emitted by radar [23]; the RCS of the nose, fuselage, and tail of the stealth UAV is smaller than conventional UAV, and the RCS value will be changed due to different radar bands and radar polarization modes. It plays an important role in the penetration path of stealth UAV in combat. For the path planning problem, RCS is usually defined as a constant, but it is not reasonable in practical application. By convention [24], it is modeled as a function of the aspect angle and roll angle as viewed from the radar. Therefore, the dynamic RCS model is adopted to an ellipsoid [1], which is given by

$$\sigma(\lambda,\theta)=\frac{\pi a^2b^2c^2}{\left(a^2\sin^2\lambda\cos^2\theta+b^2\sin^2\lambda\sin^2\theta+c^2\cos^2\lambda\right)^2}, \tag{4}$$

where σ represents the RCS value of UAV, λ represents aspect angle, θ represents roll angle, a is relatively small frontal RCS, b is a larger beam aspect RCS, and c is relatively large RCS when viewed from above or below.

3. Radar Detecting Probability

When the acquired target information meets the common track criteria, the radar system confirms the detection of the target and transmits the acquired target information to the information fusion center. The detection probability of target in a single-base radar, dual-base radar, and a radar net system is depicted as follows.

3.1. Single-Base Radar. For the single-base radar, the detection probability of the UAV is only related to the distance from the UAV to the radar center. In a period, the radar instantaneous detection probability can be expressed as follows:

$$P_t=\frac{1}{1+\left(c_2R_i^4/\sigma\right)^{c_1}}, \tag{5}$$

where P_t is the instantaneous detection probability of the single base radar, R_i is given by Eq.(2), and c_1 and c_2 are the performance parameters of specific radar, respectively.

3.2. Dual-Base Radar. The dual-base radar system is considered to be effective systems to counter the four major threats due to their technical characteristics of transmitter-receiver separation and passive reception. For the performance of the radar system, it has the advantages that single-base radar can not match, such as a larger detection range and higher accuracy. Dual-base radars are usually deployed in modern air defense systems; therefore, we focus on analyzing the dual-base radar system.

The transmitter is also employed as a receiver for dual-base radar systems, which are T/R-R systems. A transmitter can work synchronously with other splitter receivers in the dual-base radar system. The receiver synchronizes with the transmitter in time, phase, and space. The configuration of the dual-base radar system is depicted in Figure 1.

where $P(x,y)$ represents the position of the target, T represents the transmitter, R represents the receiver, D_b represents the distance between the transmitter and receiver, D_r represents the distance between the target and transmitter, D_t represents the distance between the target and receiver, and β_d represents the dual-base angle.

Additionally, D is defined as the detection range of the bistatic radar, that is $D=\sqrt{D_tD_r}$. where $D_t=\sqrt{x^2+y^2}$ and $D_r=\sqrt{(x-D_b)^2+y^2}$. D is a constant when the radar parameters are given. Hence, the maximum detection range of the bistatic radar $D_{\max}$ can be obtained by

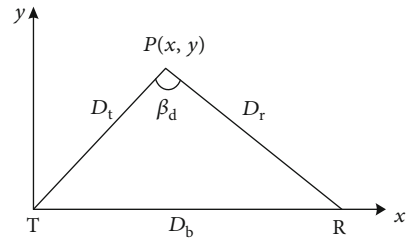

Figure 1: The configuration of the dual-base radar system.

Input: the starting point E, destination G
Output: paths
$X \leftarrow$ Min_State
While~is empty (OPEN)&&$t(X)$~ $= G$
if X = null, **then retun** to Step 1
$tag \leftarrow tag_{\min}$, delete (X)
  if $tag < h(X)$
    if $h(Y) \le tag$&&$h(X) > h(Y) + C(Y,X)$
      Calculate $h(*)$ and $f(*)$
    end
  end
  if $tag = h(X)$
    if $t(Y)$ = NEW or
      $(b(Y) = X$&$h(Y) \ne h(X) + C(X,Y))$ or
      $(b(Y) \ne X$&$h(Y) > h(X) + C(X,Y))$ **then**
      $b(Y) \leftarrow X$, Inseert$(Y, h(X) + C(X,Y))$
    end
  else
if $b(Y)$~ $= X$&&$h(Y) > h(X) + C(X,Y)$
    Insert$(X, h(X))$
  end
  else
    Insert$(Y, h(Y))$, $C(X,Y) \leftarrow$ cval
  end
  if $t(X) = E$&&$t(X)$~ = CLOSED
    Insert$(X, h(X))$; Calculate $f(*)$
  else
  return step 2
  end
end

Algorithm 1

$$D_{\max}=\left[\frac{P_\tau\sigma{\lambda_c}^2G}{(4\pi)^3KT_0L(S/N)}\right]^{1/4}, \tag{6}$$

where P_τ represents the peak power of the transmitter, G represents the antenna gain, L represents the system loss, K represents Boltzmann constant, T_0 is the noise temperature of the receiver, S/N is the signal to noise ratio of the receiver, and λ_c represents the wavelength. Similarly, the detection probability of the bistatic radar under exponential distribution is given by

$$P_D=\begin{cases}e^{-D_2/D^2{}_{\max}} & 0\le D\le D_{\max}\\ 0 & D>D_{\max}\end{cases}. \tag{7}$$

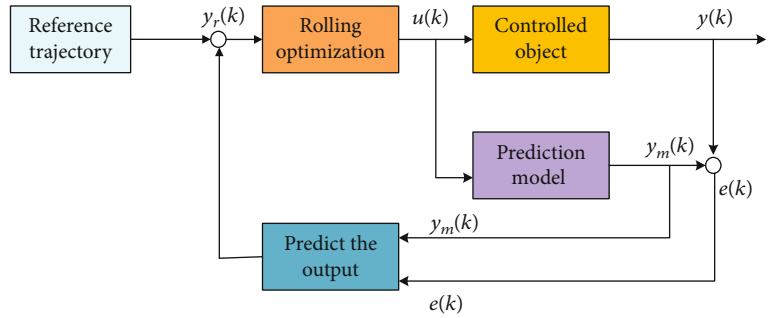

Figure 2: The principle of the MPC system.

3.3. Detection Probability of Networked Radar System. For a complete netted radar system, the radar net can improve the detection probability of UAV, significantly. The detection probability of a networked radar system mainly refers to the target detection probability calculated by the information fusion center. The rank K fusion rule is widely adopted in modern networked radar systems. Therefore, we adopt the rank K fusion rule to analyze the detection probability of networked radar [25, 26].

It is assumed that the number of radars in the netted radar system is M, which includes single-base radar and bistatic radar. When the number of radar detected in the system exceeds the detection threshold according to the rank K fusion rule, that means, the target has been detected by the radar system, and the approximate value of the optimal detection threshold K_0 can be depicted as follows.

$$K_0 = 1.5\sqrt{M}. \tag{8}$$

The radar makes a local judgment based on the detection of the stealth UAV, and the judgment results are either 0 or 1, which depends on whether the local threshold detection target exists or not. H_0 and H_1 are binary assumptions, where H_0 represents target does not exist and H_1 represents target exists. Therefore, the decision value of the jth radar ($j = 1, 2, \cdots, M$)) can be expressed as follows:

$$d_j = \begin{cases} 0 & \text{if decision result is } H_0 \\ 1 & \text{if decision result is } H_1 \end{cases}. \tag{9}$$

Additionally, the local decision result is passed to the information fusion center of the radar system to form a global decision matrix D_c, that is, $D_c = (d_1, d_2, \cdots, d_M)$. And the radar information fusion rule for the network is denoted as R; the decision rule $R(D_c)$ for rank K fusion is given by

$$R(D_c) = \begin{cases} 1 & \text{if the } \sum_{j=1}^{M} d_j \geq K_0 \\ 0 & \text{if the } \sum_{j=1}^{M} d_j < K_0 \end{cases}. \tag{10}$$

Input: the starting point E, destination G
Output: paths
$n \leftarrow (x_0, y_0), n_s \leftarrow n_{s_0} n \rightarrow$ OPEN
While~is empty(OPEN)
$f(n_s) \leftarrow h(n_s) + (1 + (\eta_i/\mu_i))k(n, n_s)$
if BB threats = 0
  if $P_{\text{Net}} < P_c$
  if n_s = G&&n_s~ = OPEN
    $n \leftarrow n_s$, $n \rightarrow$ OPEN, output paths
  else
  $n \leftarrow n_{s_i}$, **reutrn** to Step 3
else
$n_s \rightarrow$ CLOSE, **update** n and **return** to Step 3
else
Multi – Step Search
$h(n) \leftarrow \max\ \{h(n), \min_{n_s \in J}[k(n, n_s) + h(n_s)]\}$
Update the n_s**then**
$f(n_s) \leftarrow h(n_s) + (1 + (\eta_i/\mu_i))k(n, n_s)$
  Calculate σ and P_{Net}
$n \leftarrow n_s$, **update** $f(n)$ and **return** to Step 5
  end
end

Algorithm 2

Meanwhile, the total detection probability of the network radar system on the UAV is given by

$$P_{\text{Net}} = \sum_{D_c} \left[R(D_c) \prod_{d_j \in S_1} P_{d_j} \prod_{d_j \in S_0} \left(1 - P_{d_j}\right) \right], \tag{11}$$

where S_1 is a set of local decision vectors that make the fusion center judge "1", S_0 is a set of local decision vectors that make the fusion center judge "0", and P_{d_j} is the discovery probability of the first radar in the radar net.

4. Path Planning Algorithm

A-star algorithm is an effective search method to solve the shortest path in a static road network, which is widely used to settle the path planning problems of many agents. The closer the estimated distance is to the actual value, the

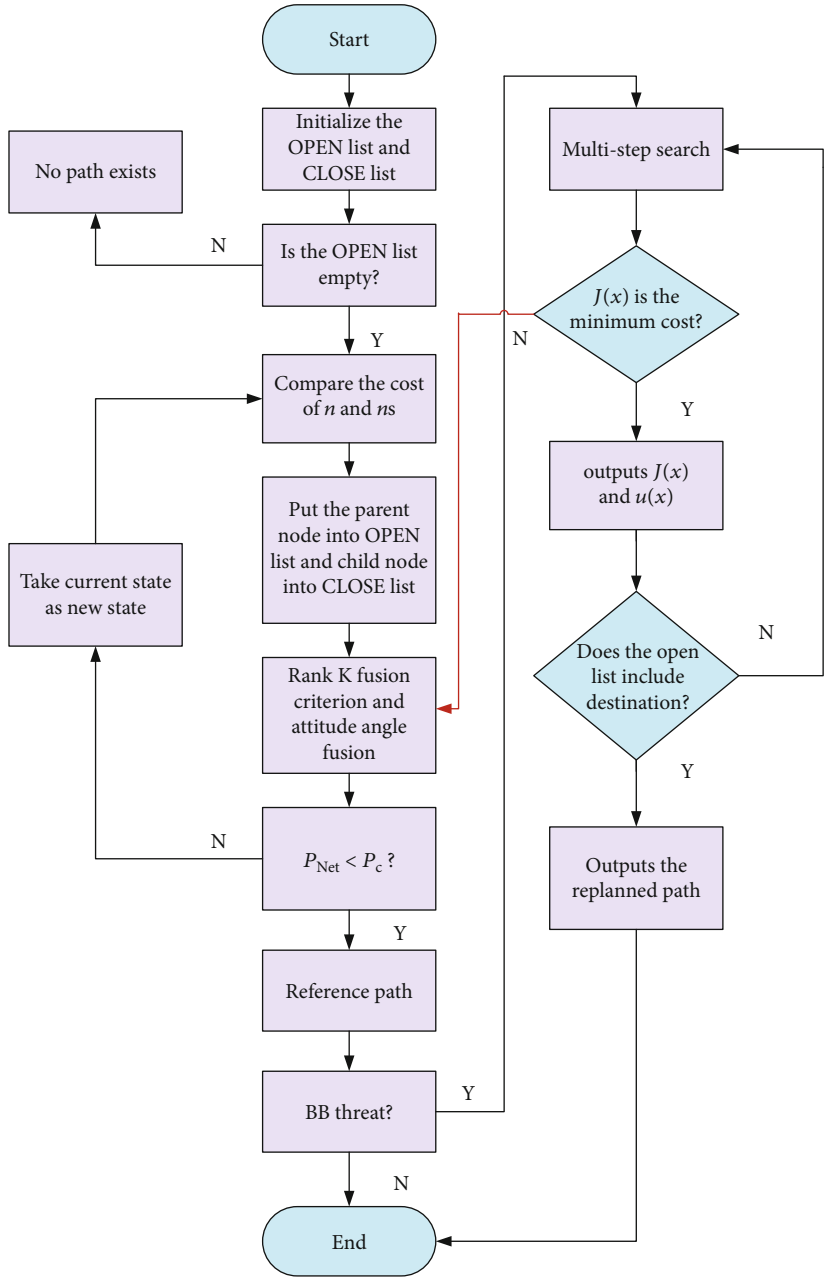

Figure 3: The flow chart of the improved A-Star algorithm.

faster the final search speed is [27–29]. This paper discusses the improvement method of the A-Star algorithm to address the penetration path planning problem for stealth UAV.

4.1. The A-Star Algorithm. The main idea of the standard A-Star algorithm is as follows. Firstly, select the appropriate heuristic function, estimate the generation value of the extensible search points in the search area, comprehensively. Moreover, compare the different cost values of each point. Moreover, consider the operation time and distance cost of the track point search. Finally, find an optimal path. In the A-Star algorithm, the operation of the OPEN list and CLOSE list are usually performed to achieve the storage and update of track points.

However, the standard A-Star algorithm that is applied to find the optimal path for stealth UAV has many disadvantages: (a) the route obtained by the A-star algorithm only has the position of stealth UAV, and it can not reflect the characteristics of the dynamic RCS and attitude angle information. (b) Unknown path cost estimation is rarely calculated in the process of path planning accurately, and the computation time is too long to find a globally optimal path. (c) the performance of real-time is poor, and the algorithm can not deal with BB threats. Therefore, we are focus on improving the performance of the A-Star algorithm.

4.2. The D-Star Algorithm. The D-Star algorithm is developed by the A-Star algorithm and the Dijkstra algorithm [30, 31], which is suitable for addressing the path planning problem in unknown environments. The main idea of the algorithm is to search the reverse path from the destination to the start, and the heuristic function expression of the D-Star algorithm is given by

$$f(X, E) = h(X) + g(X, E), \tag{12}$$

where $h(X)$ represents the actual cost of the path from the destination to state X, and $g(X, E)$ is the estimated cost of the path from the state X to the starting point.

The main steps of the D-Star algorithm are given as follows. Step 1: the value of all states are set to NEW, $f(*)$ and $h(*)$ are set to infinity for all states, $h(G)$ is set to zero, and the destination G is added to the OPEN list. Step 2: keep performing $f(*)$ the search until the location of E which is removed from the OPEN list, if the CLOSE list contains the tag value of the state X, the complete path sequence will be obtained. In contrast, path planning has failed in the threat scenario. Step 3: if the path exists, the state X can be employed to point to the destination G by the back pointer. Besides, if the $f(*)$ changes, the current path cost $C(*)$ will be immediately recalculated. Step 4: insert the affected state which near the new threat into the OPEN list, and then return to Step 2. The pseudocodes of the D-Star algorithm are depicted as follows Algorithm 1.

4.3. Improved A-Star Algorithm. We are focus on analyzing the learning real-time A-Star algorithm (LRTA-Star) which satisfies the requirements of real-time planning in a dynamic environment [32, 33]. In contrast, the path obtained by adopting the LRTA-Star algorithm is composed of a series of the tortuous track; it is difficult to achieve accurate track tracking control due to the limited maneuverability. Besides, in the flight process of stealth UAV, LRTA-Star algorithm is easy to fall into a local dead loop, which leads to the failure of path searching. Therefore, further combined with the idea of model-based predictive control (MPC) [34, 35], an improved A-Star algorithm with the multistep optimal search is proposed in this section.

MPC is an optimization control method, which is mainly composed of model prediction, feedback correction, and rolling optimization. The principle of the MPC system is depicted in Figure 2.

The closed-loop output prediction $y_p(k+1)$ is given by

$$y_p(k+1) = y_m(k+1) + h_1[y(k) - y_m(k)], \tag{13}$$

where $u(k)$ is the actual control quantity on the system at moment k, $y_r(k)$ is the reference track softened by the input filter, $y_m(k+1)$ is the predicted output value of the model, $y_p(k+1)$ is the closed-loop output prediction, and h_1 is the error correction coefficient.

Table 1: Parameters of path planning.

Parameters	Value
v	500 (km/h)
h	1 (km)
N	4
$\varphi_{\max}$	$\pi/3$
r	6 (km)
P_c	0.5
(a, b, c)	(0.317,0.178,1.000)
U	9.8 (m/s^2)
$\theta_{\max}$	$\pi/4$

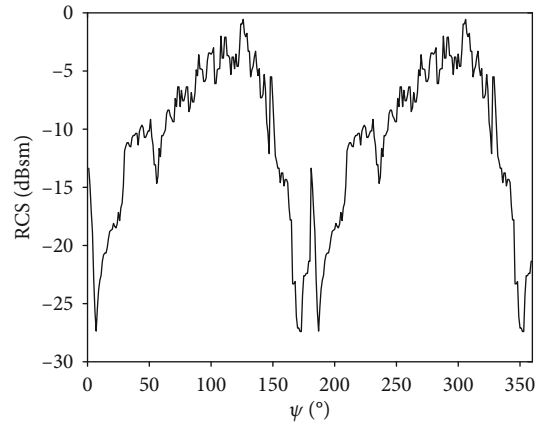

Figure 4: The RCS data of a certain type of stealth UAV.

Table 2: The geographical location and types of threat sources in the first threat scenario.

Threat	Geographic locations (km)	Type
Threat module 1	(15,10)	Known threat
Threat module 2	(25,25)	Known threat
Threat module 3	(40,35)	Known threat
Threat module 4	(30,35)	BB threat

According to Eq. (13), the optimal control law for multistep prediction is given by

$$J = \sum_{i=1}^{N} q_i \left[y_p(k+i) - y_r(k+i) \right]^2 + \sum_{j=1}^{W} \delta_j [u(k+j-1)]^2, \tag{14}$$

where N is the length of the prediction domain; W is the length of the control domain; q_i is the output prediction error, and δ_j is the weighting coefficient of the control variable.

In the process of a multistep optimization search, the track cost of each predicted track is considered as the cumulative value of the costs of N predicted track nodes. Therefore, the objective function of UAV flight path planning can be obtained according to the optimal control law of the

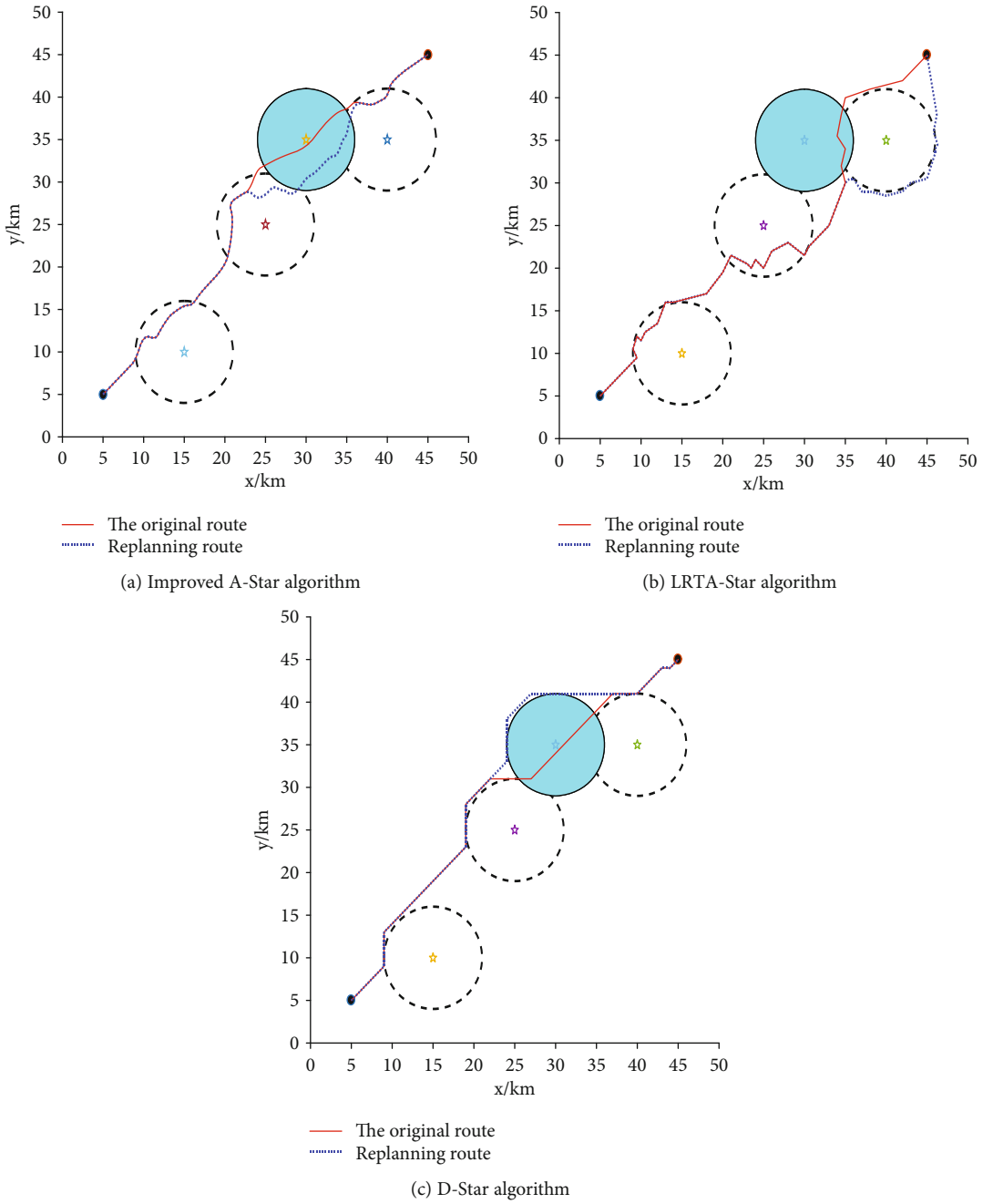

Figure 5: Numerical results of penetration path planning in the first scenario.

MPC system. The cost of the predicted flight path in N steps from the kth node is given by

$$J(k) = \sum_{j=k}^{k+N} \left[{b_1}^{\mathrm{T}}(j \mid k) B_1 b_1(j \mid k) + \varepsilon_j P_{Net}(j \mid k) \right] + \sum_{j=k}^{k+W} \delta_j u^{\mathrm{T}}(j \mid k) u(j \mid k), \tag{15}$$

where $P_{Net}(j \mid k)$ is the radar threat cost at the jth prediction point on the current predicted track segment, which can be obtained by Eq. (11). ε_j is the weight of threat cost; B_1 is the distance cost weighted matrix, $u(j \mid k)$ is the control sequence, and $b_1(j \mid k)$ is the distance cost between the coordinate of destination (x_e, y_e, h_e) and the coordinate of jth track point $[x(j \mid k), y(j \mid k), h(j \mid k)]^T$ and $b_1(j \mid k) = [x(j \mid k) - x_e, y(j \mid k) - y_e]$.

The stealth UAV is limited by its maneuverability in the process of a multistep search, where $u = (u_0, u_1, u_2, \cdots u_{N-1})$ is sought by the current track point and heading angle, and the cost function $J(k)$ for the node has a minimum value. Therefore, add the parameter $\omega (0 \le \omega \le 1)$ to the heuristic

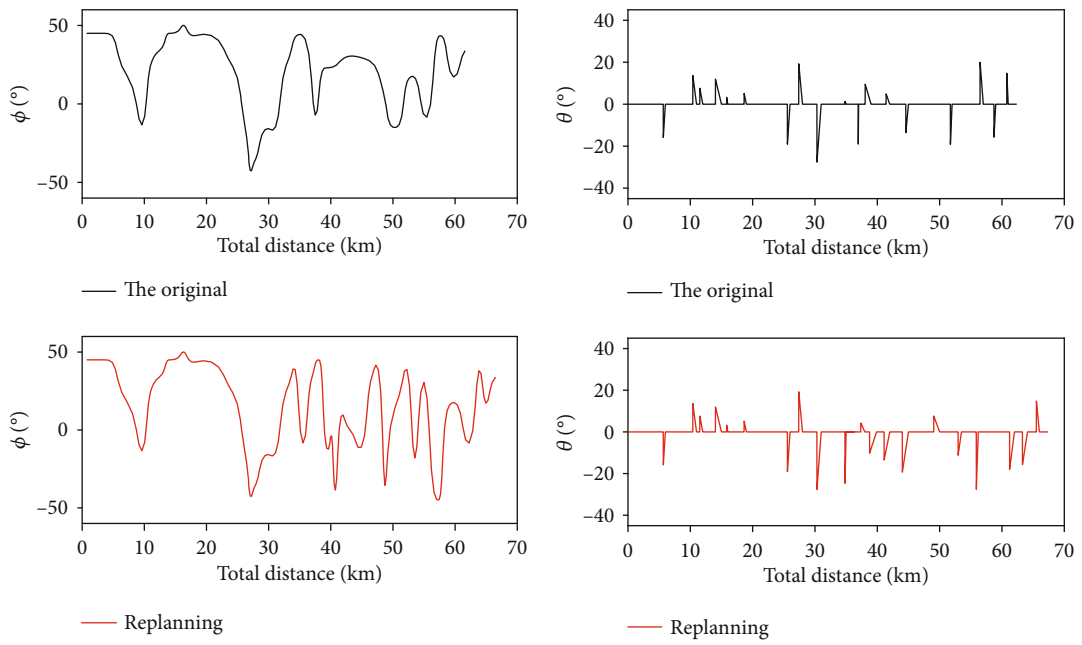

(a) The variation of heading angle (b) The variation of roll angle

Figure 6: The variation of attitude angle that performed by improved A-Star algorithm in the first scenario.

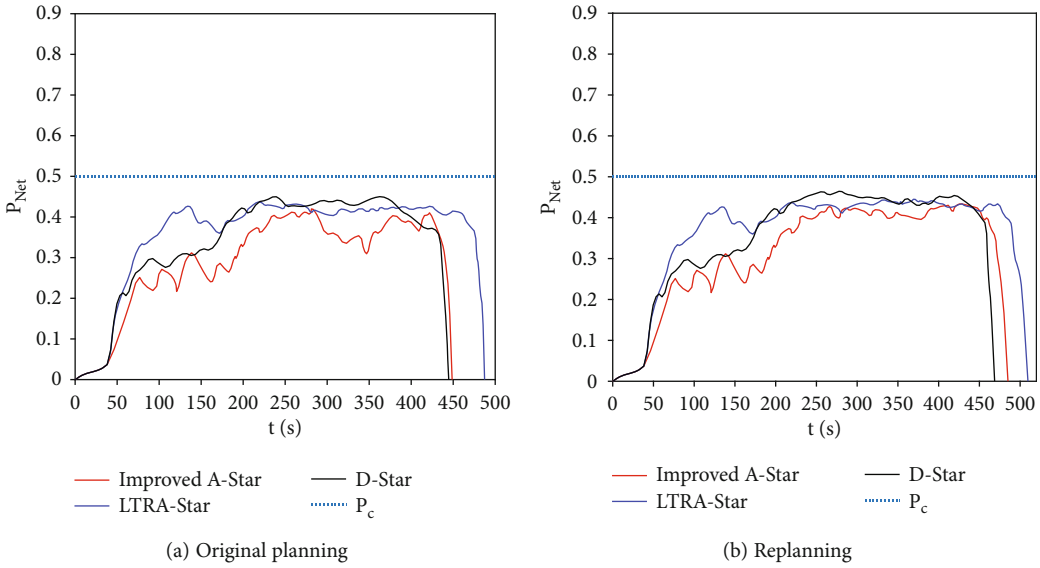

(a) Original planning (b) Replanning

Figure 7: The detection probability of netted radar in the first threat scenario.

Table 3: The statistical result of flight in the first scenario.

Situation	Algorithm	Distance (km)	P_h	Run time
Original planning	Improved A-Star	62.372	0.408	5.372
	LRTA-Star	67.743	0.418	8.276
	D-Star	61.812	0.431	8.749
Replanning	Improved A-Star	67.415	0.417	7.508
	LRTA-Star	70.833	0.429	14.624
	D-Star	65.152	0.442	13.391

Table 4: The geographical location and types of threat sources in the second threat scenario.

Threat	Geographic locations (km)	Type
Threat module 1	(15,10)	Known threat
Threat module 2	(15,20)	Known threat
Threat module 3	(40,25)	Known threat
Threat module 4	(30,35)	Known threat
Threat module 5	T (38,15), R (23,15)	Known threat
Threat module 6	(20,30)	BB threat
Threat module 7	(37,40)	BB threat

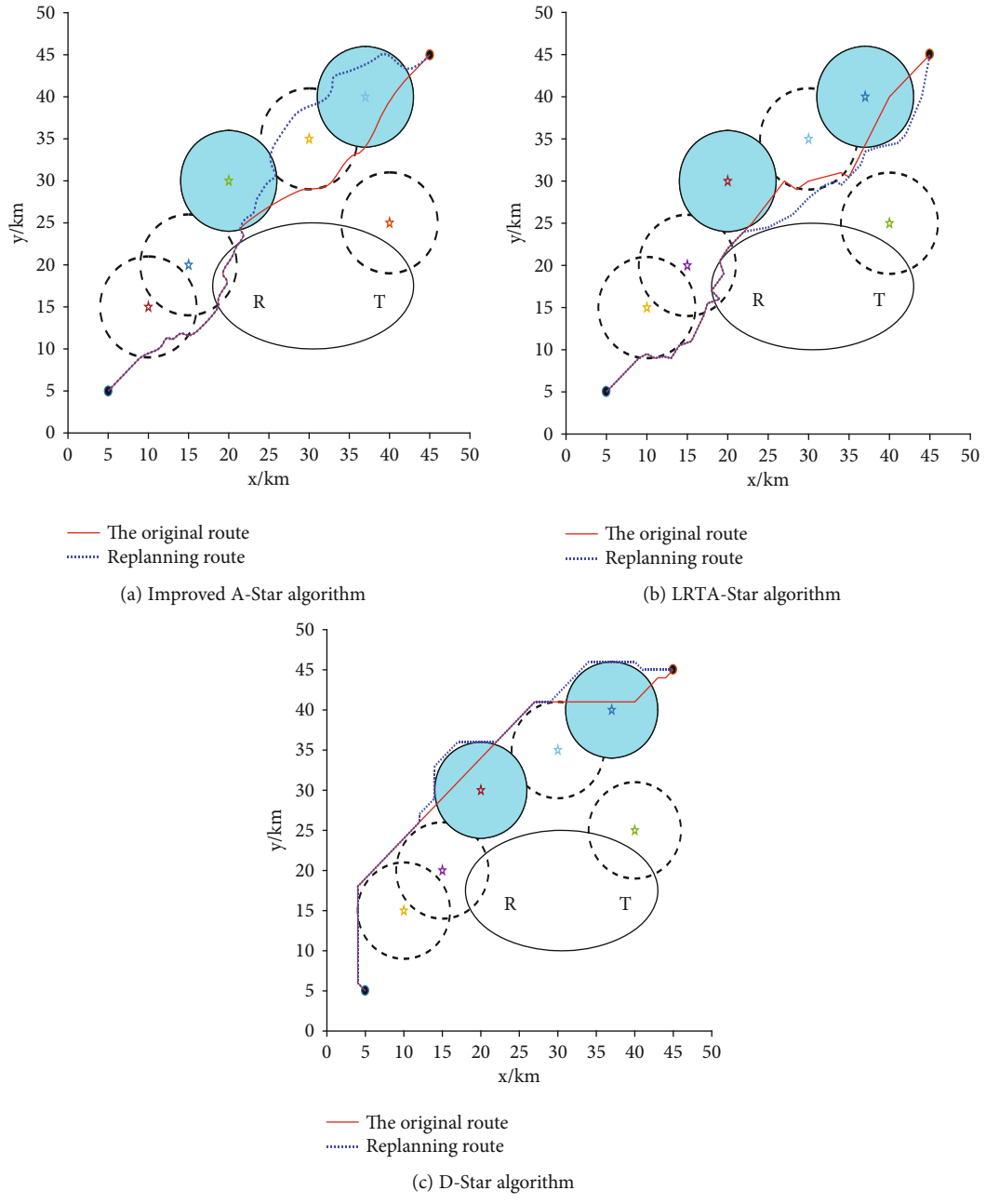

(a) Improved A-Star algorithm

(b) LRTA-Star algorithm

(c) D-Star algorithm

Figure 8: Numerical results of penetration path planning in the second scenario.

function of the original algorithm, which aims to simplify the operation, reduce the search time and ensure the optimality of path planning, and the new heuristic function expression in the improved A-Star algorithm is given by

$$f(n_s) = h(n_s) + \left(1 + \frac{\eta_i}{\mu_i}\right) k(n, n_s). \tag{16}$$

Where η_i/μ_i is the ratio of the path cost of the current state to the path cost of an unknown region, n is the current node, n_s is the adjacent extended node, and $k(n, n_s)$ is the cost from the current node to the adjacent node, and $k(n, n_s) = g(n_s) - g(n)$. The pseudocode of the improved A-Star algorithm is depicted as follows Algorithm 2, and the flow chart of the improved A-Star algorithm is depicted in Figure 3.

5. Numerical Results

Numerical simulations of penetration path planning are performed by employing the improved A-Star algorithm, LRTA-Star algorithm, and D-Star algorithm in different threat scenarios, which aims to verify the effectiveness of the improved A-Star algorithm. The simulation experiments are conducted with MATLAB2020Ra software and a Windows 10 system. The parameters of flight are depicted in Table 1, the value K_0 is determined by the number of radar M, and it will change when there is a BB threat in the threat scenario.

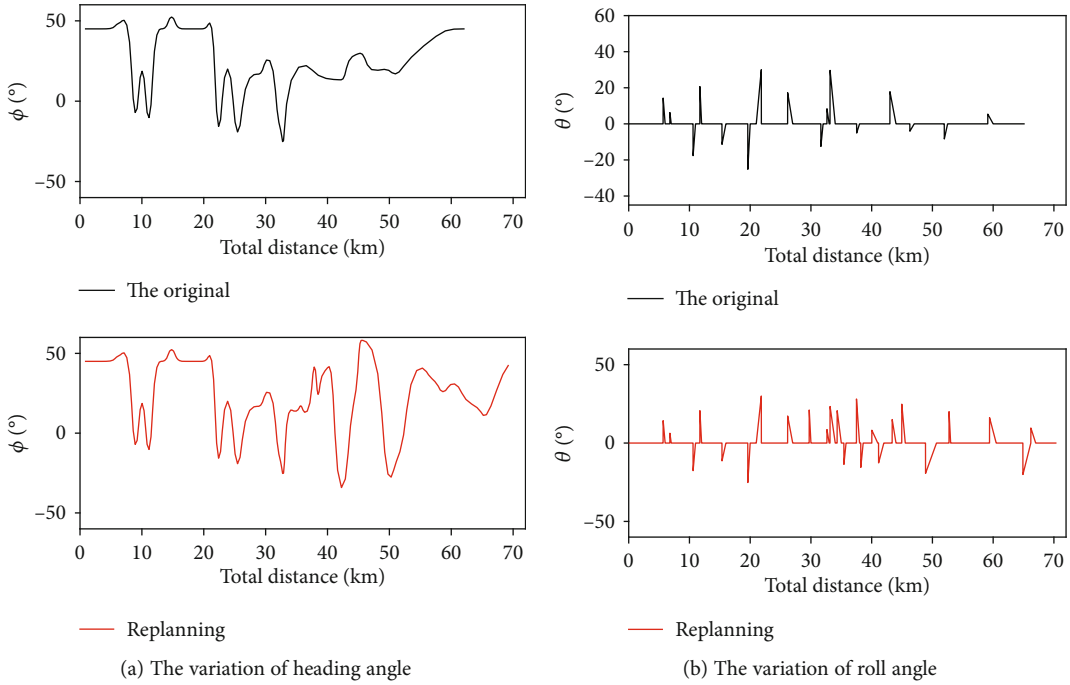

(a) The variation of heading angle

(b) The variation of roll angle

FIGURE 9: The variation of attitude angle employed by improved A-Star algorithm in the second scenario.

Additionally, it is considered as the probability state of radar high detection when P_{Net} exceeds 0.4, and P_h is performed to evaluate the safety degree of the track segment. The RCS data of a certain type of stealth UAV is depicted in Figure 4.

5.1. The First Threat Scenario. The threat region has a range of 50 km × 50 km; the geographical location and types of threat sources are presented in Table 2. The coordinate of the starting point is (5,5) km, and the coordinate of the target point is (90,90) km. The numerical results of penetration path planning which is performed by different algorithms in the first scenario are depicted in Figure 5. The variation of heading angle and roll angle which is applied by the improved A-Star algorithm in the first scenario is depicted in Figure 6, the detection probability of netted radar in the first threat scenario is depicted in Figure 7, and the statistical result of flight in the first scenario is presented in Table 3.

Figure 5 demonstrates the penetration paths for stealth UAV which is performed by employing three different algorithms in a scenario. From Figure 7 and Table 3, we can infer that the stealth UAV can achieve penetration path planning by employing in the first scenario in which a static or dynamic environment. However, compared with the other two algorithms, the paths obtained by employing the improved A-Star algorithm has a smaller value of P_h and takes less time. Figure 6 demonstrates that the improved A-Star algorithm can accurately adjust the attitude angle and reduce the value of RCS on the paths, and this algorithm achieves the rapid and safe path penetration planning for stealth UAV. Besides, the paths of the improved A-Star algorithm is shorter than the LRTA-Star algorithm, and the improved A-Star algorithm has higher path planning efficiency and safety, which further proves the effectiveness of the improved A-Star algorithm.

5.2. The Second Threat Scenario. The threat region has a range of 50 km × 50 km; the geographical location and types of threat sources are presented in Table 4. The coordinate of the starting point is (5,5) km, and the coordinate of the target point is (90,90) km. The numerical results of penetration path planning which is performed by different algorithms in the second scenario are depicted in Figure 8. The variation of heading angle and roll angle which is performed by an improved A-Star algorithm in the second scenario is depicted in Figure 9, the detection probability of netted radar in the second threat scenario is depicted in Figure 10, and the statistical result of flight in the second scenario is presented in Table 5.

Figure 8 describes the penetration paths for stealth UAV which is performed by applying three different algorithms in a scenario with more complex threat sources, and from Figure 10 and Table 5. For the original path planning, the penetration paths which are safe by employing all three algorithms in the scenario. However, for the path replanning in the presence of BB threats, the path replanning has failed in the second threat scenario, because the P_h of paths by adopting the LRTA-Star algorithm and D-star algorithm are higher than 0.5. Inversely, stealth UAV can still achieve the path replanning in the second scenario with two BB threats by using an improved A-Star algorithm. Moreover, the improved A-Star algorithm takes less time and has higher path planning efficiency than the other two algorithms whether in the original path planning or replanning, and it further proves the validity of the algorithm. Figure 9 indicates that when the improved A-Star algorithm is performed to

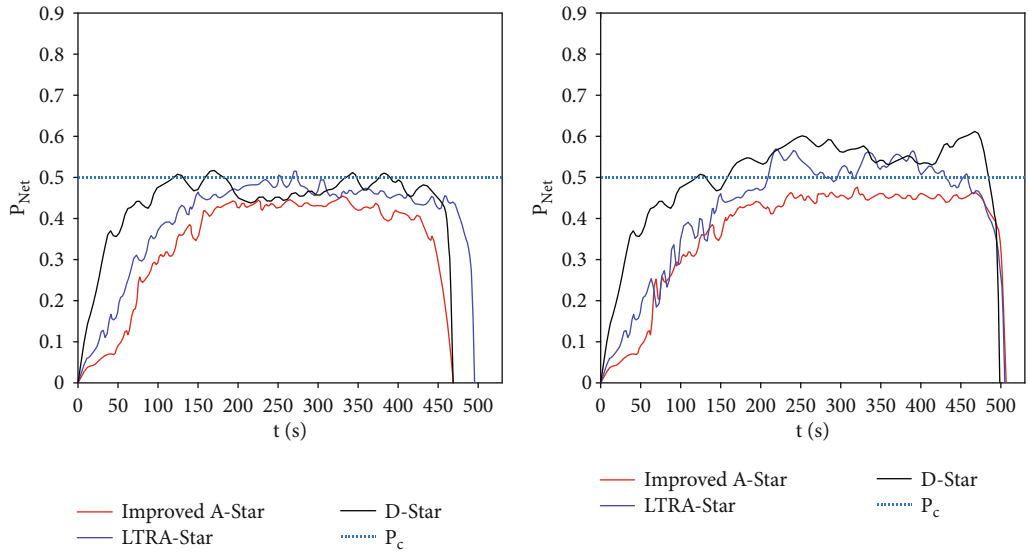

(a) Original planning

(b) Replanning

Figure 10: The detection probability of netted radar in the second threat scenario.

Table 5: The statistical result of flight in the second scenario.

Situation	Algorithm	Distance (km)	P_h	Run time
Original planning	Improved A-Star	65.192	0.429	6.053
	LRTA-Star	68.879	0.459	10.504
	D-Star	65.152	0.470	11.581
Replanning	Improved A-Star	70.425	0.446	9.827
	LRTA-Star	70.191	0.502	16.117
	D-Star	69.321	0.535	18.659

penetration path planning, the variation of heading angle and roll angle are within the preset range, which can satisfy the real flight requirements.

5.3. The Third Threat Scenario. The threat region has a range of 50 km × 50 km; the geographical location and types of threat sources are presented in Table 6. The coordinate of the starting point is (5,5) km, and the coordinate of the target point is (90,90) km. The numerical results of penetration path planning which is performed by different algorithms in the third scenario are depicted in Figure 11. The variation of heading angle and roll angle which is performed by an improved A-Star algorithm in the third scenario is depicted in Figure 12, the detection probability of netted radar in the third threat scenario is depicted in Figure 13, and the statistical result of flight in the third scenario is presented in Table 7.

Figure 11 describes the penetration paths for stealth UAV which are performed by applying three different algorithms in a scenario with a large number of threat sources and BB threats; from Figure 13 and Table 7, we can see that the P_h paths by adopting the LRTA-Star algorithm and D-star algorithm are higher than 0.5 no matter in the original path planning or path replanning. Obviously, stealth UAV can rarely achieve the penetration path planning which is safely and rapidly by employing these two algorithms. However, the P_h of paths by adopting improved A-Star algorithms are always lower than 0.5; therefore, stealth UAV can still achieve penetration path planning and replanning by using the improved A-Star algorithm in dynamic threat scenarios. Furthermore, paths of the improved A-Star algorithm have higher efficiency and safety, which further proves the validity of the improved A-Star algorithm in the scenario with high threat density. Figure 12 indicates that stealth UAV can meet constraints of attitude angle in the field of close and low altitude combat.

Table 6: The geographical location and types of threat sources in the third threat scenario.

Threat	Geographic locations (km)	Type
Threat module 1	(7,22)	Known threat
Threat module 2	(15,30)	Known threat
Threat module 3	(40,20)	Known threat
Threat module 4	(26,35)	Known threat
Threat module 5	(37,40)	Known threat
Threat module 6	(44,30)	Known threat
Threat module 7	(12,40)	Known threat
Threat module 8	(42,12)	Known threat
Threat module 9	T (33,13), R (15,13)	Known threat
Threat module 10	(30,25)	BB threat
Threat module 11	(20,42)	BB threat
Threat module 12	(33,43)	BB threat

6. Conclusions

This paper presented a new solution for path replanning for stealth unmanned aerial vehicle in a complex radar net environment with BB threats.

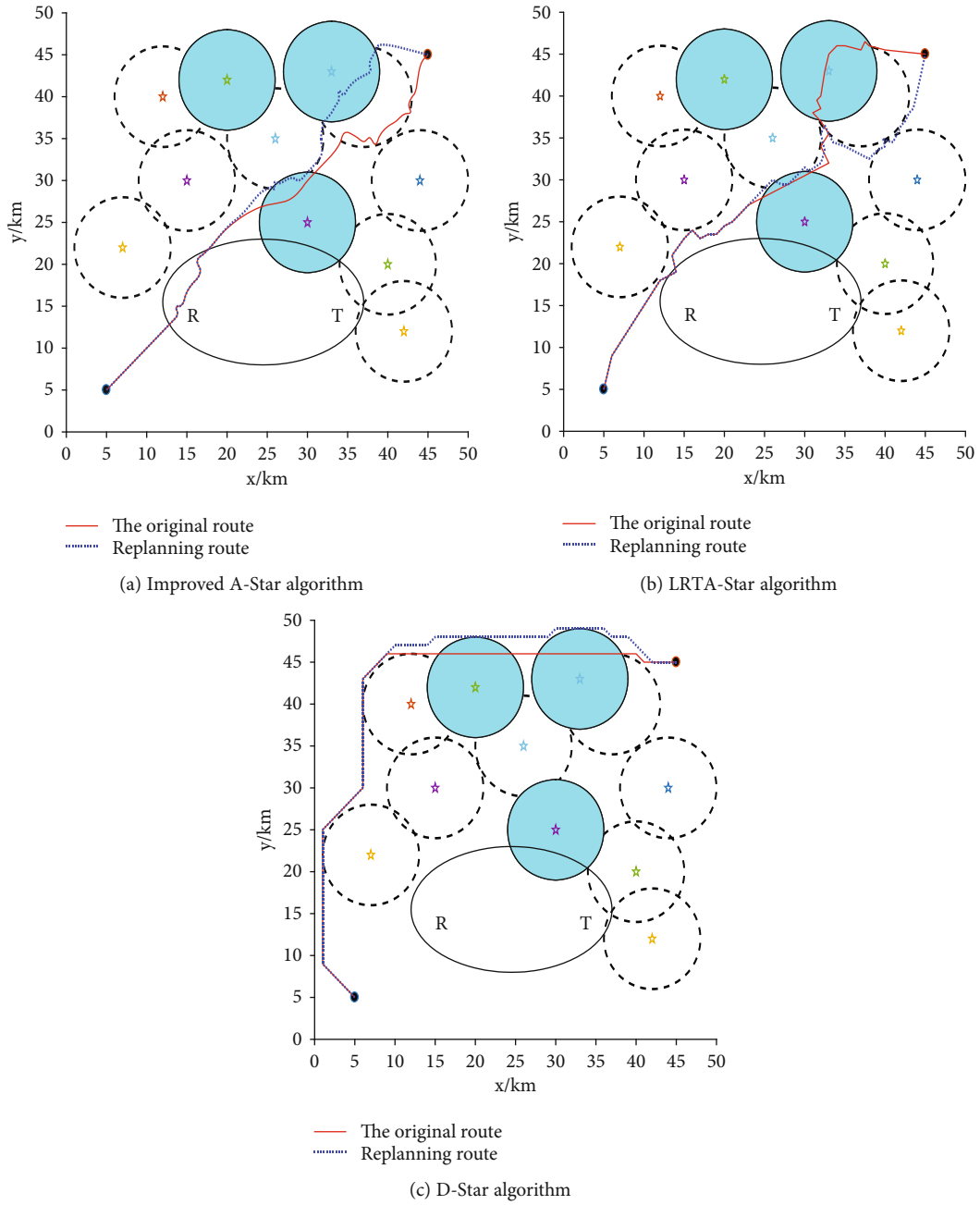

(a) Improved A-Star algorithm

(b) LRTA-Star algorithm

(c) D-Star algorithm

Figure 11: Numerical results of penetration path planning in the third scenario.

We are focus on analyzing the kinematics model of stealth UAV, threat source in penetration environment, and path planning algorithm. Further combined with model-based predictive control (MPC) and the LRTA-Star algorithm, an improved A-Star algorithm is proposed to achieve penetration path planning and replanning for stealth UAV. Meanwhile, the attitude angle information of stealth UAV is added to the algorithm, which demonstrates the variation characteristics of dynamic RCS. Further combined with the kinematics analysis of stealth UAV and the detection performance analysis of radar net, the original paths, and the replanning paths can satisfy the real flight requirements.

Compared with the other two algorithms, the stealth UAV can rapidly achieve the penetration path planning by employing the improved A-Star algorithm in a different complex environment with BB threats, improve the survivability of stealth UAV, and the efficiency of penetration path planning.

The threat scenarios are composed of single-base radar, dual-base radar, and BB threats, which are closer to the real combat environment. The model and the improved A-Star algorithm proposed in this paper can quickly generate better penetration paths in the combat area under a dynamic environment, exhibiting certain military application value.

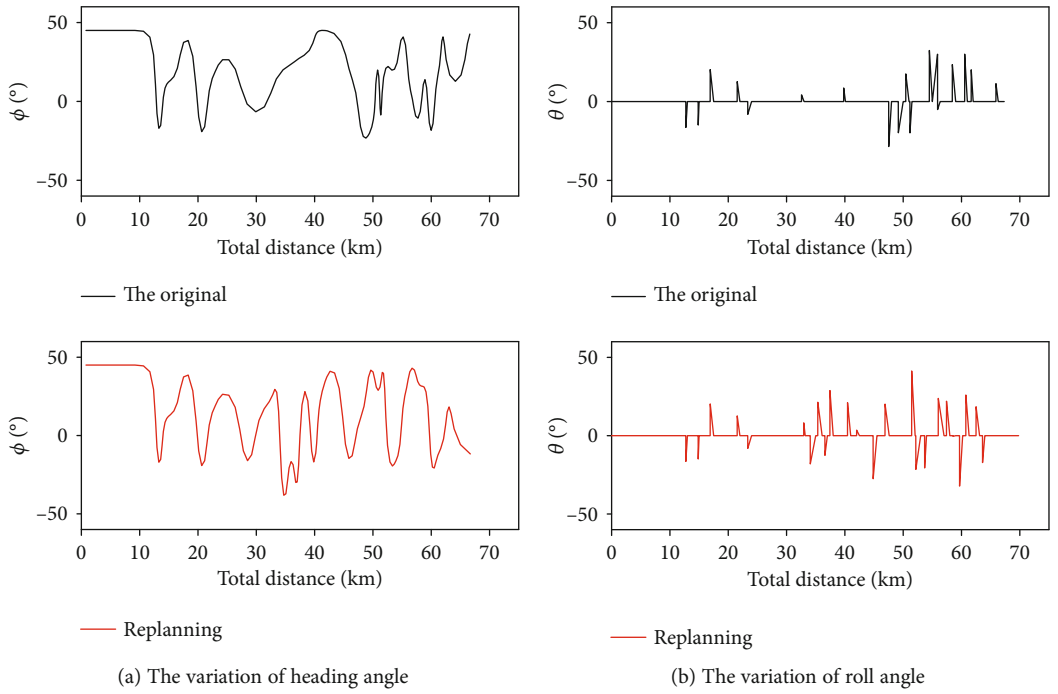

(a) The variation of heading angle

(b) The variation of roll angle

Figure 12: The variation of attitude angle that performed by improved A-Star algorithm in the third scenario.

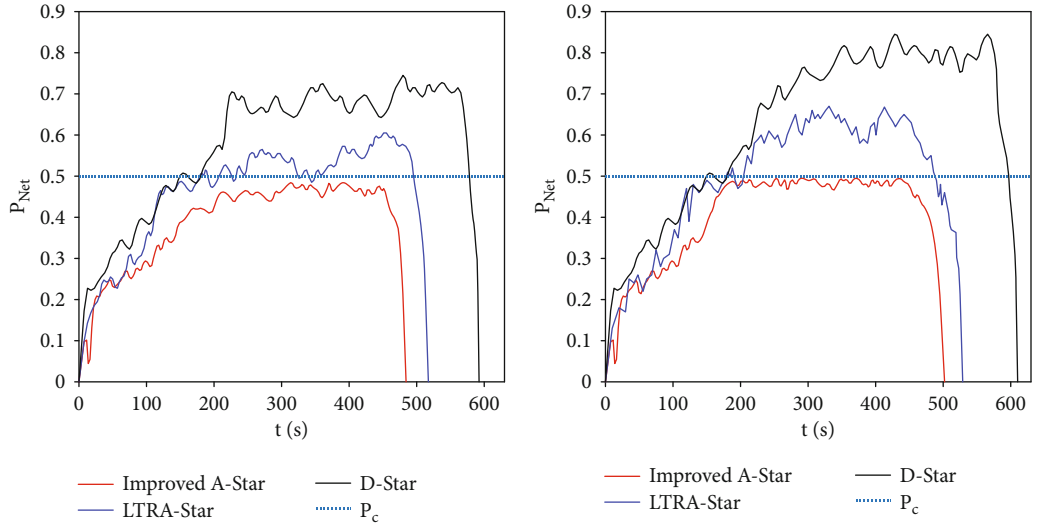

(a) Original planning

(b) Replanning

Figure 13: The detection probability of netted radar in the third threat scenario.

Table 7: The statistical result of flight in the third scenario.

Situation	Algorithm	Distance (km)	P_h	Run time
Original planning	Improved A-Star	67.316	0.457	9.259
	LRTA-Star	71.909	0.521	16.746
	D-Star	82.339	0.639	19.468
Replanning	Improved A-Star	69.788	0.476	17.362
	LRTA-Star	73.520	0.570	28.732
	D-Star	84.825	0.698	34.085

In future work, we are focus on the real-time rapid penetration path planning for stealth UAV account for a three-dimensional complex dynamic environment with the terrain and unknown motion targets in the field of close and low altitude combat.

Data Availability

No data were used to support this study.

Conflicts of Interest

The authors declare that there is no conflict of interest regarding the publication of this paper.

Acknowledgments

This work was supported in part by the National Natural Science Foundation of China under grant 61663032, Aeronautical Science Foundation of China under grant 2016ZC56003, and Innovation Special Fund of Nanchang Hangkong University for Graduate Student under grant YC2019026.

References

[1] F. H. Zeitz III, "UCAV path planning in the presence of radar guided surface to air missile threats, [Ph.D. dissertation]," Dept. Elect.Eng., University of Michigan, Detroit, MI, USA, 2005.

[2] B. Yan, R. Liu, P. Dai, M. Xing, and S. Liu, "A rapid penetration trajectory optimization method for hypersonic vehicles," *International Journal of Aerospace Engineering*, vol. 2019, Article ID 1490342, 11 pages, 2019.

[3] E. Sepulveda and H. Smith, "Technology challenges of stealth unmanned combat aerial vehicles," *The Aeronautical Journal*, vol. 121, no. 1243, pp. 1261–1295, 2017.

[4] F. W. Moore, "Radar cross-section reduction via route planning and intelligent control," *IEEE Transactions on Control Systems Technology*, vol. 10, no. 5, pp. 696–700, 2002.

[5] T. Inanc, M. K. Muezzinoglu, K. Misovec, and R. M. Murray, "Framework for low-observable trajectory generation in presence of multiple radars," *Journal of guidance, control, and dynamics*, vol. 31, no. 6, pp. 1740–1749, 2008.

[6] Q. Xu, J. Ge, and T. Yang, "Optimal Design of Cooperative Penetration Trajectories for Multiaircraft," *International Journal of Aerospace Engineering*, vol. 2020, Article ID 8490531, 12 pages, 2020.

[7] H. Liu, J. Chen, L. Shen, and S. Chen, "Low observability trajectory planning for stealth aircraft to evade radars tracking," *Proceedings of the Institution of Mechanical Engineers, Part G: Journal of Aerospace Engineering*, vol. 228, no. 3, pp. 398–410, 2014.

[8] S. Chen, H. Liu, J. Chen, and L. Shen, "Penetration trajectory planning based on radar tracking features for UAV," *Aircraft Engineering and Aerospace Technology*, vol. 85, no. 1, pp. 62–71, 2013.

[9] J. J. Ruz, O. Arévalo, M. Jesús, and G. Pajares, "Using MILP for UAVs trajectory optimization under radar detection risk," in *Proceedings of the IEEE Conference on Emerging Technologies and Factory Automation 2006*, pp. 957–960, Prague, Czech Republic, 2006.

[10] R. Wang and J. Liu, "Adaptive formation control of quadrotor unmanned aerial vehicles with bounded control thrust," *Chinese Journal of Aeronautics*, vol. 30, no. 2, pp. 807–817, 2017.

[11] J. Zhang, Q. Hu, D. Wang, and W. Xie, "Robust attitude coordinated control for spacecraft formation with communication delays," *Chinese Journal of Aeronautics*, vol. 30, no. 3, pp. 1071–1085, 2017.

[12] T. Erlandsson, "Route planning for air missions in hostile environments," *The Journal of Defense Modeling and Simulation: Applications, Methodology, Technology*, vol. 12, no. 3, pp. 289–303, 2015.

[13] T. Erlandsson and L. Niklasson, "Automatic evaluation of air mission routes with respect to combat survival," *Information Fusion*, vol. 20, pp. 88–98, 2014.

[14] A. Le, V. Prabakaran, V. Sivanantham, and R. Mohan, "Modified a-star algorithm for efficient coverage path planning in tetris inspired self-reconfigurable robot with integrated laser sensor," *Sensors*, vol. 18, no. 8, 2018.

[15] M. A. Mohammed, M. K. Abd Ghani, R. I. Hamed, S. A. Mostafa, M. S. Ahmad, and D. A. Ibrahim, "Solving vehicle routing problem by using improved genetic algorithm for optimal solution," *Journal of Computational Science*, vol. 21, pp. 225–262, 2017.

[16] Y. Lu, Z. Xue, G. S. Xia, and L. Zhang, "A survey on vision-based UAV navigation," *Geo-spatial Information Science*, vol. 21, no. 1, pp. 21–32, 2018.

[17] A. Majeed and S. Lee, "A fast global flight path planning algorithm based on space circumscription and sparse visibility graph for unmanned aerial vehicle," *Electronics*, vol. 7, no. 12, p. 375, 2018.

[18] Y. Li, R. Cui, Z. Li, and D. Xu, "Neural network approximation based near-optimal motion planning with kinodynamic constraints using RRT," *IEEE Transactions on Industrial Electronics*, vol. 65, no. 11, pp. 8718–8729, 2018.

[19] S. Shao, Y. Peng, C. He, and Y. du, "Efficient path planning for UAV formation via comprehensively improved particle swarm optimization," *ISA Transactions*, vol. 97, pp. 415–430, 2020.

[20] Y. Zhao, Z. Zheng, and Y. Liu, "Survey on computational-intelligence-based UAV path planning," *Knowledge-Based Systems*, vol. 158, pp. 54–64, 2018.

[21] P. Kumar, S. Garg, A. Singh, S. Batra, N. Kumar, and I. You, "MVO-Based 2-D path planning scheme for providing quality of service in UAV environment," *IEEE Internet of Things Journal*, vol. 5, no. 3, pp. 1698–1707, 2018.

[22] A. Bakdi, A. Hentout, H. Boutami, A. Maoudj, O. Hachour, and B. Bouzouia, "Optimal path planning and execution for mobile robots using genetic algorithm and adaptive fuzzy-logic control," *Robotics and Autonomous Systems*, vol. 89, pp. 95–109, 2017.

[23] A. Laučys, S. Rudys, M. Kinka et al., "Investigation of detection possibility of UAVs using low cost marine radar," *Aviation*, vol. 23, no. 2, pp. 48–53, 2019.

[24] C. Fang, "The simulation and analysis of quantum radar cross section for three-dimensional convex targets," *IEEE Photonics Journal*, vol. 10, no. 1, pp. 1–8, 2018.

[25] C. Fang, H. Tan, Q.-F. Liu et al., "The calculation and analysis of the bistatic quantum radar cross section for the typical 2-D plate," *IEEE Photonics Journal*, vol. 10, no. 2, pp. 1–14, 2018.

[26] C. Zhang, X. Jiang, and D. Chen, "RCS promotion in orbital angular momentum imaging radar with rotational antenna," *IET Radar, Sonar & Navigation*, vol. 13, no. 12, pp. 2140–2144, 2019.

[27] F. Duchoň, A. Babinec, M. Kajan et al., "Path planning with modified a star algorithm for a mobile robot," *Procedia Engineering*, vol. 96, pp. 59–69, 2014.

[28] C. Liu, Q. Mao, X. Chu, and S. Xie, "An improved A-star algorithm considering water current, traffic separation and berthing for vessel path planning," *Applied Sciences*, vol. 9, no. 6, p. 1057, 2019.

[29] Y. Li, T. Ma, P. Chen, Y. Jiang, R. Wang, and Q. Zhang, "Autonomous underwater vehicle optimal path planning method for seabed terrain matching navigation," *Ocean Engineering*, vol. 133, pp. 107–115, 2017.

[30] T. T. Mac, C. Copot, D. T. Tran, and R. D. Keyser, "A hierarchical global path planning approach for mobile robots based on multi- objective particle swarm optimization," *Applied Soft Computing*, vol. 59, pp. 68–76, 2017.

[31] F. A. Raheem and U. I. Hameed, "Path planning algorithm using D∗ heuristic method based on PSO in dynamic environment," *American Scientific Research Journal for Engineering, Technology, and Sciences*, vol. 49, no. 1, pp. 257–271, 2018.

[32] K. Singh, K. Singh, L. H. Son, and A. Aziz, "Congestion control in wireless sensor networks by hybrid multi-objective optimization algorithm," *Computer Networks*, vol. 138, pp. 90–107, 2018.

[33] Y. Zhao, S. Yin, D. Li, Q. Yu, and P. Ranjitkar, "Improving motorway mobility and environmental performance via vehicle trajectory data-based control," *IEEE Access*, vol. 8, pp. 86862–86869, 2020.

[34] Z. Zhang, J. Wu, J. Dai, and C. He, "A novel real-time penetration path planning algorithm for stealth UAV in 3D complex dynamic environment," *IEEE Access*, vol. 8, 2020.

[35] A. Afram, F. Janabi-Sharifi, A. S. Fung, and K. Raahemifar, "Artificial neural network (ANN) based model predictive control (MPC) and optimization of HVAC systems: a state of the art review and case study of a residential HVAC system," *Energy and Buildings*, vol. 141, pp. 96–113, 2017.